Applied Surface Science 289 (2014) 358–365

Contents lists available at ScienceDirect

Applied Surface Science

journal homepage: www.elsevier.com/locate/apsusc

Electron irradiation-enhanced water and hydrocarbon adsorption in EUV lithography devices

A. Al-Ajlony*, A. Kanjilal[1], M. Catalfano, S.S. Harilal, A. Hassanein

Center for Materials Under Extreme Environment, School of Nuclear Engineering Purdue University, West Lafayette, IN 47907, USA

ARTICLE INFO

Article history:
Received 19 August 2013
Received in revised form
24 September 2013
Accepted 28 October 2013
Available online 8 November 2013

Keywords:
EUV lithography
Adsorption
Au surface
Secondary electrons
Assisted adsorption

ABSTRACT

The accumulation of water and hydrocarbons molecules on pure Au smooth surfaces were monitored during 100 eV electron bombardment at various beam current levels. Our studies showed that these low energy electrons could accelerate the physical adsorption processes of the gaseous contaminant molecules on the mirror surface. The 100 eV electron beam was used to provide a rough simulation of the secondary electrons generated during the interaction between the EUV beam at 13.5 nm wavelength and the mirror surface in an EUVL device. The adsorption enhancement phenomenon was explained in accordance with Langmuir's Adsorption model by the increase of the sticking coefficient of adsorbed molecules onto the mirror surface. We have also shown that a positive biasing of the top of mirror surface can be used for preventing the secondary electron emission from the mirror surface.

1. Introduction

Due to the escalating demands on new advancement of computer chips specifications, including microprocessors and integrated circuits and for keeping Moore's law intact, the number of transistors per unit area [1] must be increased in about every two years. Nowadays we almost reached the theoretical limit of the conventional optical lithography for further reduction in feature size with a reasonable resolution [2,3]. Several next generation lithography (NGL) technologies are now being considered [2,3]. In fact, extreme ultraviolet lithography (EUVL) is considered to be the most promising technology among the others of NGL techniques [4]. EUVL is not only a promising tool, but also very challenging considering the technological point of view. Although huge progress has been achieved so far to ease many of these challenges [4], many issues are yet to be sorted out and hence still under intense research. Some of these obstacles that partially contribute to the delay in commercializing the EUVL device are the lack of powerful and clean EUV source [4], the difficulty of achieving defect free photo-mask [4], and carbon contamination of the EUV optics [5,6].

Carbon contamination in EUV optics is caused by EUV induced dissociation of the hydrocarbon molecules at the mirror surface during irradiation [7,8]. This dissociation process eventually leads to the formation of amorphous graphite like carbon layer that reduces the EUV reflectivity of the mirrors [8,9]. Basically, the hydrocarbon molecules (gaseous phase) accumulate naturally on the mirror surface, which is known (so far) to be independent of the EUV irradiation process [5,10]. During mirror exposure to the EUV radiation, these stable molecules can be dissociated to smaller reactive fragments that react with each other to form eventually carbon rich solid layer [5,11,12].

Generally, the accumulation of gaseous molecules on top of solid surfaces is one of the possible interactions between solid and gaseous phases, known as the adsorption process [13]. The adsorption process occurs due to the ability of gaseous molecules to be bonded physically (physisorption) or chemically (chemisorption) on a solid surface and stay there for a period of time until it has sufficient energy to break the bond and desorb back to the gaseous phase [13]. The mean lifetime of the gaseous molecules bonded to the solid surface and the number of events that lead to successful sticking of one gaseous molecule on solid surface are the two main factors that determine the equilibrium concentration of the adsorbed phase at certain conditions [13]. Back in 1918, Langmuir had established one of the first adsorption theories based on kinetic point of view, determining the equilibrium concentration of adsorbed phase of certain system (adsorbent and adsorbates) at certain pressure and temperature, leading to his famous isotherm [13,14]. Langmuir's findings lead to numerous advanced theories and empirical relations to match a variety of experimental data at different conditions [13]. It is known, however, that the

* Corresponding author. Tel.: +1 7654091695.
E-mail address: aalajlon@purdue.edu (A. Al-Ajlony).
[1] Present address: Department of Physics, School of Natural Sciences, Shiv Nadar University, Uttar Pradesh 203207, India.

0169-4332/$ – see front matter © 2013 Elsevier B.V. All rights reserved.
http://dx.doi.org/10.1016/j.apsusc.2013.10.167

assumption behind the Langmuir theory for single monomolecular-layer adsorption is not precise enough for many practical applications [13,15]. Moreover, the smooth uniform surface that was suggested as adsorbent in Langmuir theory is too ideal for most of the practical cases [13]. On the other hand, the Langmuir adsorption theory is reasonably precise enough when considering the adsorption process of gases on extremely smooth solid surface under high vacuum or ultra-high vacuum (UHV) atmosphere where the partial pressure of the adsorbates is not high enough to produce a monolayer of adsorbed molecules on the surface. These conditions are applicable in the case of water and hydrocarbon adsorption on mirror surface in EUVL devices.

The physical adsorption process on a mirror surface in the case of pure component adsorption system is known to be exclusively dependent on the partial pressure of the adsorbates and the temperature of the adsorbing surface [13–15]. An increase in adsorption rate of gaseous species on certain surfaces after exposing them to a flux of energetic electrons had been reported [16–18]. This phenomenon was explained in the framework of the role of energetic electrons to induce dissociation of adsorbed molecules, where the produced reactive fragments can react chemically with the surface to produce more stable chemical bonds (chemisorption) [16]. This chemical effect increases the mean lifetime of the adsorbates on the surface, leading eventually to an increase in the adsorption rate [16,17].

In this paper we report the impact of 100 eV electron beam on the physisorption of hydrocarbons and H_2O on a relatively inert surface (Au). The main goal of this paper is to present the role of secondary electrons in enhancing the adsorption process on a reflecting EUV mirror during EUV exposure. It should be pointed out that the adsorption process is the early and the governing stage that dictate the rate of the subsequent dissociation stages. Therefore, it governs the entire contamination processes and feature the EUV induced contamination process in the future EUVL device. This article is designed to provide a systematic view of the early stages of the surfaces contamination process from a kinetic point of view. The 100 eV electrons were chosen to provide a rough simulation of the electrons generated during the mirror exposure to 92 eV EUV radiation which corresponds to the wavelength of next generation lithography [12,19,20]. These generated electrons together with the reflected EUV beam are expected to reach the subsequent mirrors in a lithographic system and accelerate the contamination process. Although Au is not a favorable candidate materials to cap the Si/Mo multilayer mirrors (MLMs) for the EUVL device [10,21], it was however used in this experiment to provide a relatively inert surface that cannot easily react with the adsorbates species. Hence, we can reduce any possible chemisorption processes. Also Au surface was selected to avoid any interference in X-ray photoelectron spectroscopy (XPS) spectral lines with the C 1*s* line, providing a good opportunity to monitor the accumulation of the hydrocarbons on the surface. Currently Ru is considered as a capping layer for Mo/Si multilayer mirror and it is difficult to monitor the accumulation of hydrocarbons on the top of Ru using XPS due to the overlapping between the C 1*s* and Ru 3*d* lines [5,22–24].

2. Experimental details

A set of (10 mm × 10 mm) 50 nm thick Ru and Au films coated Si wafers was used in this investigation. All these samples were studied in an UHV chamber (base pressure $\sim 3.0 \times 10^{-9}$ Torr) in the materials characterization laboratory IMPACT [25] at Purdue University. For each sample, surface contamination level was evaluated by XPS analysis, where sample's surface was excited with Al-K_α radiation ($h\nu$ = 1486.6 eV), while the photoelectrons emitted at 45° from the target surface were analyzed using a hemispherical

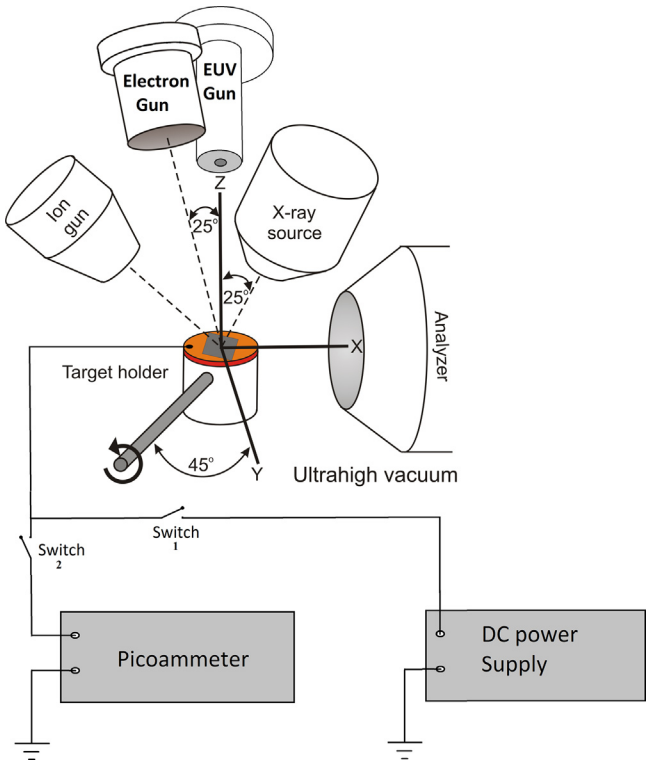

Fig. 1. The schematic of the experimental setup. The IMPACT system is used which contains X-ray source, electron gun, ion gun, EUV source, and hemispherical electrostatic energy analyzer. A dc power supply was used to bias the sample surface positively or negatively and a picoammeter was used to measure the target current.

electrostatic energy analyzer (PHOIBOS-100^{TM}). Calibration of binding energy (BE) scale with respect to the measured kinetic energy was made using the Au $4f_{7/2}$ line at ~84.00 eV. A set of three experiments was devoted to study the dynamics of contaminants concentration at the sample surface in different experimental conditions as summarized in the next two sections. During all experiments, chamber pressure was fixed at $\sim 1.0 \times 10^{-8}$ Torr in order to simulate the optics chamber pressure of an EUVL system [26]. The schematic of the experimental setup is given in Fig. 1 with different electrical switch configuration for each part of the experiment.

2.1. Effect of electron bombardment

In this part of the experiment, Au samples were used. The sample surface was examined by XPS at different time intervals to monitor the level of surface contaminants during electron bombardment at different beam currents. Before electron beam bombardment, Au samples were sputter cleaned for 10 min by 1 keV Ar^+ with a total beam current of ~0.5 μA using an ion source from NTI^{TM}. Immediately after sputter cleaning, sample was irradiated by 100 eV electron beam from a SPECS^{TM} electron gun. During electron bombardment a series of high resolution XPS scans were taken for O 1*s*, C 1*s* and Au 4*f* core regions. The experiment was repeated for different electron beam currents (860 nA and 220 nA) and also in the absence of electron bombardment (e-beam off). In the case of the electron beam off, the electron source filament was also kept off. The experimental setup of this part is presented in Fig. 1 with the switches 1 and 2 were in off and on positions, respectively.

2.2. Secondary electron emission mitigation

In this experiment, Ru samples were used. The samples were biased with different positive voltages during 92 eV EUV irradiation, and effect of sample bias voltage on the surface emitted secondary electron (SE) spectra was studied. The electrical switches configuration for this part of the experiment as mentioned in Fig. 1, switch 1 was in on position while switch 2 was off. The EUV irradiation was performed using a Phoenix^{TM} EUV source [27] that emits light in the range of 12.5–15 nm with the maximum peak at ~13.5 nm. The estimated EUV beam power reaching the target surface is ~0.3 μW, while the power of the 13.5 nm wavelength of light (within 2% bandwidth) is ~0.1 μW [25,27]. The EUV beam spot size on the investigating Ru surface was estimated to be ~7 mm. Although the EUV beam power in our EUV source is significantly lower than the actual EUV beam power intended for the future EUVL device, the kinetic energy distribution of the S.Es generated using both sources will be approximately similar, and only the intensity will be different. The SE spectrum was recorded using PHOIBOS-100 hemispherical electrostatic energy analyzer.

In addition, we also investigated the impact of sample biasing on the adsorption process of contaminants on the Au surface. Initially, the Au samples were sputter cleaned for 10 min by 1 keV Ar+ with a total beam current of ~0.5 μA. Immediately after sputter cleaning, the Au samples were biased positively or negatively at different voltages and a series of high resolution XPS scans were taken for the O 1*s* and C 1*s* regions. In this experiment +200, +100, −40 and 0 V were applied during each experimental run.

3. Results and discussion

3.1. Effect of electron bombardment

A polished "mirror like" Au samples were sputter cleaned and immediately bombarded with low energy electrons (100 eV) at different currents (860 nA, 220 nA and e-beam off). At the same time, a series of XPS scans were taken to measure the level of contamination on the sample surface with time. Fig. 2 gives the C 1*s*, O 1*s* and Au 4*f* peaks which show the natural accumulation (e-beam off) of contaminants on Au mirror surface with time. In this case no electron bombardment was carried on, and only the accumulation of contaminants on the sample surface due to the normal adsorption of the residual gaseous species in the vacuum chamber is observed. As can be seen in Fig. 2, the O 1*s* core level spectrum does not show significant signal right after sputtering, but with time the oxygen concentration at the surface starts to build up. By careful looking into this region and to the position of the oxygen peak formed at around 533 eV we can conclude that this peak is corresponding to the adsorbed water molecules at the surface [5,10,12,22,24]. The measured partial pressure of water in our chamber was ~2.0×10^{-9} Torr during the experiments.

Along with O 1*s* core peak, we also monitored C 1*s* (Fig. 2(b)) and the results showed the carbon signal is also increasing with time. In fact, the carbon peak found to be positioned at 284.8 eV which is the most accepted value for the adventitious hydrocarbons [5,10,24] that could be adsorbed at any metallic surface due to the presence of residual hydrocarbons in a vacuum chamber atmosphere [10]. This observation also justified by the adsorption process of the hydrocarbons on the sample surface. Although the sample was sufficiently clean at the moment of stopping the sputter cleaning process, the first scan of the C 1*s* region after cleaning shows the presence of carbon. It indicates that carbon accumulation happens immediately after sputter cleaning. This carbon is most likely accumulated by surface adsorption of hydrocarbons during the first ~2 min which is required to complete an XPS scan.

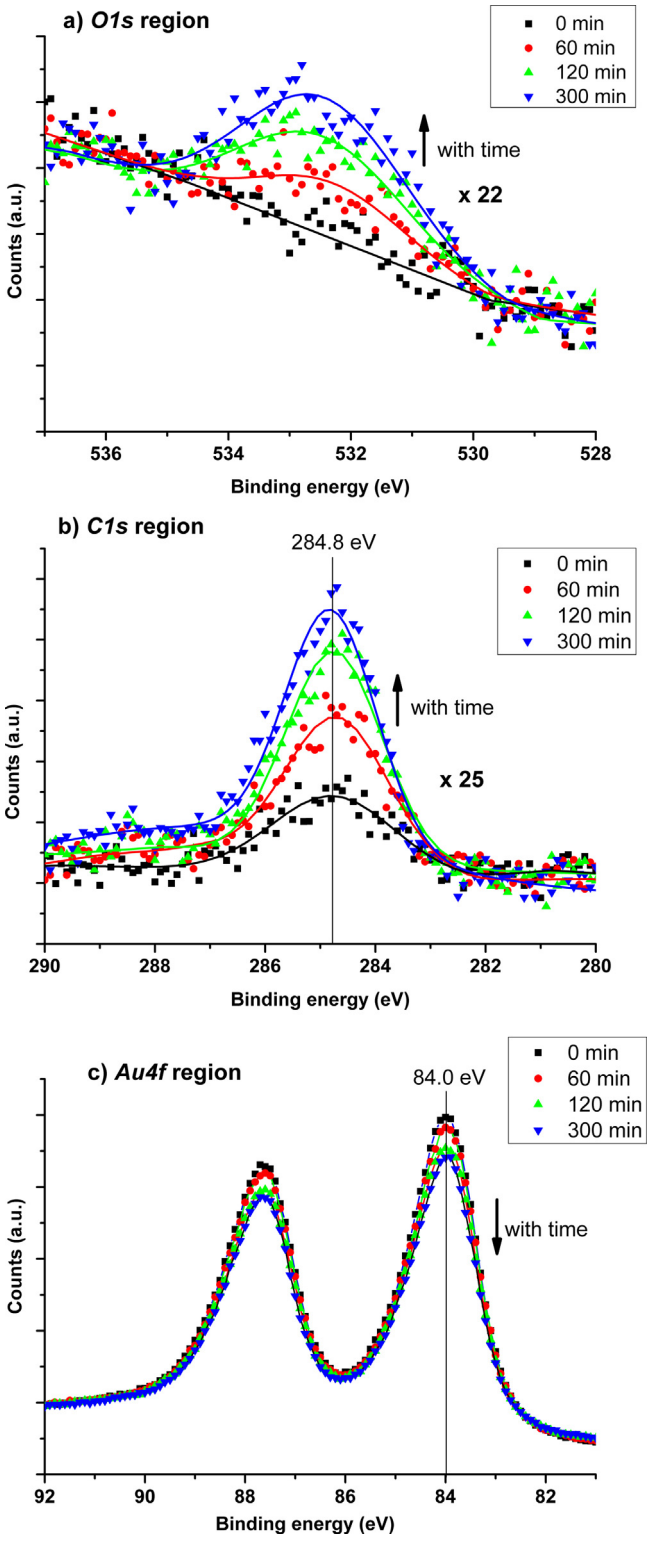

Fig. 2. High resolution XPS spectra of (a) O 1*s*, (b) C 1*s* and (c) Au 4*f* core level peaks. The XPS scans were performed in 1-h intervals starting from sputtered clean surface.

We also monitored time dependent changes in the Au 4*f* core level peak (Fig. 2(c)), which shows a continuous decrease in Au surface concentration. The decrease in intensity of Au signal confirms that the observed contaminants, especially H_2O and hydrocarbons were accumulating and covering the Au surface. The suppression of

the Au signal also supports our hypothesis of surface contamination via molecular adsorption.

The behavior of contaminant adsorption was also studied during low energy electron bombardment. Fig. 3 gives the temporal evolution of the area under the XPS spectra at the O 1*s* (H_2O), C 1*s* (hydrocarbon), and Au 4*f* regions during the contamination process under different electron beam currents (860 nA and 220 nA) as well as for the natural adsorption process (e-beam off). Fig. 3(a) shows significant change in H_2O adsorption rate during the electron bombardment process. The electron bombardment has increased the rate of H_2O adsorption at the surface where the adsorption rate was found to change with electron current. For a beam current of 220 nA, the surface water concentration reaches the saturation in a shorter time period ~120 min compared to ~240 min required without electron bombardment. For 860 nA electron current, the H_2O surface saturation reached even faster ~50 min. Interestingly, the water concentration was also decreased steadily after reaching the saturation point when the electron bombardment was used. This slow but linear decrease of water concentration after saturation was previously noticed during EUV irradiation [5,10] and it was justified therein by the dissociation of water molecules due to SE-induced dissociation process. At the same time no decrease in water concentration after saturation was found when the electron bombardment was not applied (not shown).

Similar change in adsorption behavior during electron bombardment was also noticed in the C 1*s* region as can be seen in Fig. 3(b). In this region we noticed a dramatic increase in adsorption rate of hydrocarbon at sample surface during electron bombardment, and this increase was directly proportional to electron beam current. This increase in adsorption rate resulted in shortening of the time required for hydrocarbons to reach saturation at the sample surface compared to the time of saturation when the electron beam was not applied. Moreover, in the case of electron bombardment carbon concentration was found to be steadily increased with a very slow rate even after saturation. This gradual increase in carbon was also noticed during the EUV irradiation [5,10] and it was justified therein by the accumulation of carbon due to the SE-assisted hydrocarbon dissociation process.

The time dependent behavior of Au signal is given in Fig. 3(c) which confirms the role of electron bombardment in modifying surface adsorption rate. The Au signal was decreased at a faster rate when the electron bombardment was in use. Based on our observations in all XPS regions studied (such as O 1*s*, C 1*s* and Au 4*f*), the surface concentrations of all contaminants at equilibrium (the saturation level) were not found to be significantly altered when the electron bombardment was applied. Although the adsorption rate was found to be significantly increased during electrons bombardment, the saturation concentration at the surface was found to be approximately similar. We noticed a significant increase in adsorption rate of water and hydrocarbons on Au mirror surface during low energy electron exposure. The same phenomenon had been observed repeatedly for different adsorption systems [16–18]. For example, the adsorption of nitrogen on nickel was increased significantly during low energy electron bombardment, especially at electron energies higher than 15 eV [16]. This phenomenon was explained by the effect of electrons in dissociating the N_2 molecules and allowing the N fragment to interact with the adsorbent surface [16]. The use of XPS in the present experiment allows us to recognize the chemical state of adsorbates. The recorded XPS spectra showed no evidence of additional Au chemical state or any shift of the Au pure state (Au^0). Based on this stability of Au^0, we can conclude that all changes of adsorption rates were not based on a chemical interaction between the adsorbed molecules and the Au surface, and all adsorption process noticed was basically a physisorption. We used Langmuir theory to explain some of the observed phenomena.

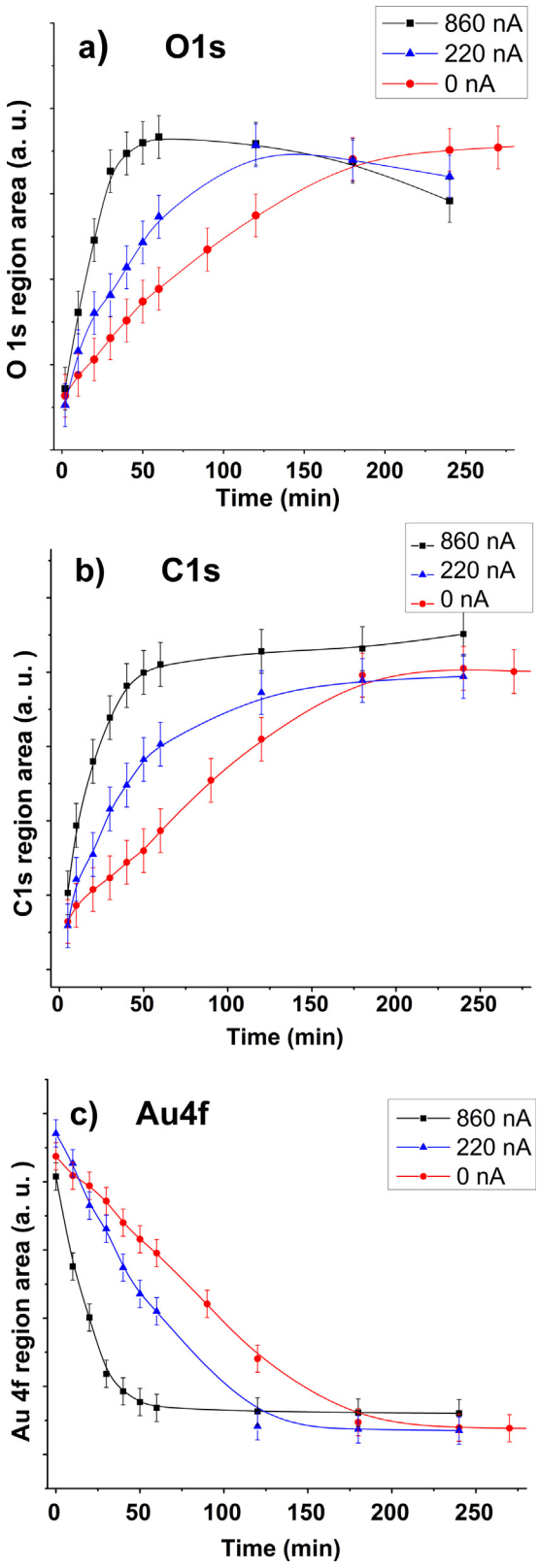

Fig. 3. Temporal evolution of the area under XPS spectrum of the (a) O 1*s* region, (b) C 1*s* region, and (c) Au 4*f* region. The curves highlight the evolution of the surface concentration of oxygen (H_2O), carbon, and Au during 100 eV electron bombardments for different currents. The corresponding natural evolution in the absence of electron bombardment (0 nA) is also shown.

Langmuir theory of pure component physical adsorption is based on a very simple explanation of the adsorption process as mentioned in Eq. (1). This denotes the time rate of change of total number of adsorbed molecules which is equal to the rate of adsorption R_a (i.e. the number of molecules successfully bonded to the surface per unit of time) minus the rate of desorption R_d (i.e. number of bonded molecules that leave the surface per unit time) [13,14]

$$\frac{dn}{dt} = R_a - R_d$$

$$R_a = \frac{\alpha P}{\sqrt{2\pi M R_g T}}(1-\theta)$$

$$R_d = k_{d\infty}\ \exp\left(-\frac{E_d}{R_g T}\right)\theta \tag{1}$$

where $\theta = n/m$, n is the number of adsorption sites occupied by the adsorbates, m is the number of available adsorption site on the adsorbent, α is sticking coefficient of the adsorbed molecule onto a bare surface, P is the partial pressure of the adsorbates, M is the molar mass of the adsorbed molecules, R_g is the universal gas constant, T is the surface temperature, $k_{d\infty}$ is the rate constant of desorption at temperature equal to ∞, E_d is the activation energy for desorption.

The Langmuir isotherm [13,14] can be obtained at equilibrium when $R_a = R_d$, leading to:

$$\theta = \frac{bP}{1+bP}$$

$$\text{where}\quad b = \frac{\alpha \exp(-E_d/R_g T)}{k_{d\infty}\sqrt{2\pi M R_g T}} \tag{2}$$

In UHV atmosphere, the partial pressure of the adsorbed molecules is very low ($\sim 10^{-11}$ Torr). Therefore, the fractional coverage at equilibrium can be achieved with minimal adsorbed molecules at the surface. Furthermore, the Langmuir adsorption theory assumptions of a single monomolecular layer can be reasonably accurate.

For non-equilibrium case, Eq. (1) represents a constant coefficient first order differential equation that can be solved for $n(t)$ by taking into account the initial condition $n = 0$ at $t = 0$. Therefore, the solution can be obtained as follows:

$$n(t) = A\left(1 - \exp\left(\frac{-\alpha P}{A\sqrt{2\pi M R_g T}}\right)\right),$$

$$A = \frac{m\alpha P}{\alpha P + k_{d\infty}\ \exp(-E_d/R_g T)\sqrt{2\pi M R_g T}} \tag{3}$$

where A is a constant, representing the number of adsorbed molecules at the surface at equilibrium ($t = \infty$). The function $n(t)$ can strongly justify the exponential behavior of the accumulation of the adsorbed molecules on the Au surface with time as shown in Fig. 3, especially in the case where no electrons were applied to the surface. Adding electrons to the surface can only increase the adsorption rate by either increasing the sticking coefficient (α) and/or by increasing the activation energy for desorption (E_d). It should be noted that the effect of any change in α on the adsorption rate is more dominant at earlier times of adsorption, while the effect of any change in E_d is more effective at later time and it has a maximum value at equilibrium. From Fig. 3 it is clear that, the electrons bombardment has increased the adsorption rate in the earlier time, while it causes a decrease in the adsorption rate at later time or near the equilibrium concentration. Hence, we can conclude that the electron bombardment of the Au surface enhances the adsorption rate of both water and hydrocarbon molecules by increasing α. The increase in α can be explained by the role of electrons in creating a temporary positively charged gaseous molecules, and by creating a negatively charged Au surface due to the fact that the electron yield of the Au surface is less than 1 for 100 eV incident electrons, which is proven by our negative sample current measurement at 100 eV. Hence, the electrostatic force between the positively charged gaseous molecules and the negatively charged surface increases the chance of sticking of these molecules onto the surface. At the same time this electrostatic force is not expected to have any role on E_d since the positive charge of the adsorbed molecules will be neutralized immediately once the adsorbed molecules touch the surface due to the abundance of free electrons on the Au surface.

On the other hand, as can be understood from the decrease of the adsorption rate at later time of adsorption, the electron bombardment of the Au surface was found to decrease E_d. This phenomenon can be explained by the SE induced dissociation process that splits the larger adsorbed molecules into smaller fragments, which in turn can be desorbed easily from the surface (i.e. the smaller fragment molecules will require less energy to leave the surface back to the gaseous phase).

More careful analysis was made for the C 1*s* region because of the importance of the carbon contamination of the EUV mirrors in EUVL systems. The main carbon peak in the C 1*s* region situated at 284.8 eV was found to be composed of mainly two different chemical states [28,29] as presented in Fig. 4(a). Graphitic carbon line or C—C line was found to be situated at 284.5 eV [28,29], and C—H line was found to be situated at 285.4 eV [28,29]. The temporal evolution of the surface concentration of these two carbon components is presented in Fig. 4(b). In this figure we compare the behavior of the two carbon components on the Au surface with and without electron bombardment. As can be seen clearly, both components (C—H and C—C) were found to follow the same trend observed for total carbon (see Fig. 3(b)). Also we noticed that in both cases (with and without electron bombardment) the increase in C—C component was faster and stronger than the C—H component, which implies that heavy hydrocarbon molecules with multiple carbon atoms were being accumulated on the Au surface. Also a slight increase in C—C component was noticed after saturation only when the electron bombardment was in use, while C—H component was found to be unchanged.

3.2. Secondary electron emission mitigation

As discussed in the previous sections, a large number of secondary electrons are emitted from the EUV irradiated mirror surface. The energy distribution of these electrons varies from the kinetic energy of the incident photons to 0 eV [19]. The lower energy part of this spectrum (also called SE) is produced due to a slowing down process of the high kinetic energy photoelectrons that undergo cascade collisions with other stationary lattice electrons. While the higher kinetic energy electrons are generally produced due to direct interaction of a photons with valence electrons that bonded with the lattice atoms with a minimum BE. These emitted secondary electrons are also expected to interact with the next mirror surface posing further contamination in addition to the primary contamination process caused by the EUV photons themselves.

Assuming all electrons is generated due to the interaction between the EUV light and the mirror surface (photoelectrons and secondary electrons). These electrons problem can be overcome by biasing the mirror surface positively at a voltage that is sufficient to create electrical field to decelerate the produced electrons and totally mitigate the notorious electron emission. We recorded the photoelectron spectrum emitted by Ru mirror surface irradiated

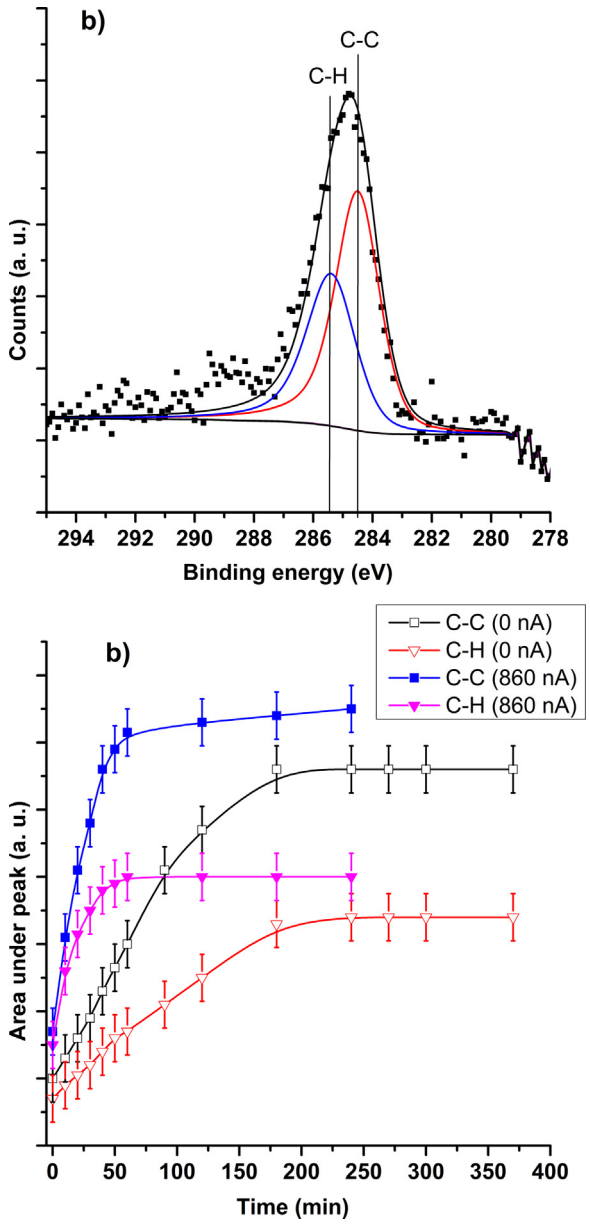

Fig. 4. The peak fitting of high resolution XPS spectrum of (a) C 1*s* region of the Au surface. (b) The temporal evolution of the area under the peak of both components of the C 1*s* region C—C and C—H during 100 eV electron bombardment for electron beam current of about 860 nA. The temporal evolution of the same components in the absence of electron bombardment (0 nA) are also superimposed for comparison.

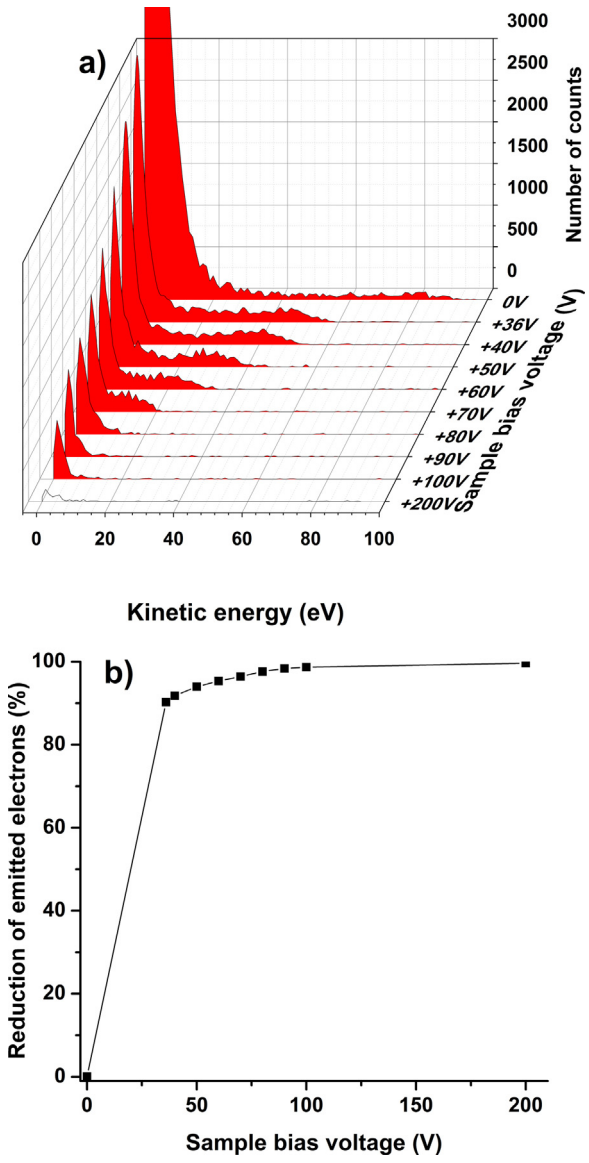

Fig. 5. (a) The impact of surface bias voltage on the SE spectrum emitted from Ru surface during 13.5 nm wavelength EUV irradiation. (b) The percentage of the reduction of the emitted electrons from the Ru surface irradiated by 13.5 nm EUV versus surface bias voltage.

by 13.5 nm (92 eV) at various sample positive bias voltages in order to check the effectiveness of biasing to mitigate the SE emission. As shown in Fig. 5(a), it can be seen clearly that the positive bias of the sample largely reduces the intensity of electron emission and shifts the whole spectrum toward the lower kinetic energy side. Converting these data to a mitigation percentage, Fig. 5(b) shows that the biasing the Ru surface by +36 V mitigates 90% of the emitted electrons and reduced the maximum electrons kinetic energy by 36 eV. Meanwhile, biasing the surface by +100 and +200 V mitigates more than 98% and 99% of the emitted electrons, respectively, and reduces the maximum electron kinetic energy to less than 10 eV. Based on these results, we can conclude that the positive biasing of the mirror surface is useful for mitigating the SE emission, and that in turn would be advantageous for reducing the overall contamination rate in a stack of several mirrors in the EUVL device.

Now the next question is what is the effect of the surface biasing on the surface adsorption mechanism? Since the surface charging can cause changes in adsorption rate. For answering this question, Au surface was sputter cleaned and immediately biased at different voltages, while a series of XPS scans were recorded to track the temporal evolution of surface composition. We examined the natural accumulation of the water and hydrocarbons at the mirror surface through the adsorption process, and neither electrons nor EUV radiations were involved in this contamination process. Fig. 6 shows the accumulation of both H_2O (O 1*s*) and hydrocarbons (C 1*s*) with time at the top of Au surface at various sample bias voltages. As can be seen from Fig. 6, changing the surface bias voltage and polarity does not have a significant impact on the H_2O accumulation, and that is also identical to what we have noticed in the first part of the experiment (in the case of electron beam off), where H_2O contamination level saturates after about 200 min. A slight increase in rate of H_2O accumulation was noticed when the sample was biased by −40 V and this can be justified by the sensitivity of the H_2O as a polar molecule to the negatively charged

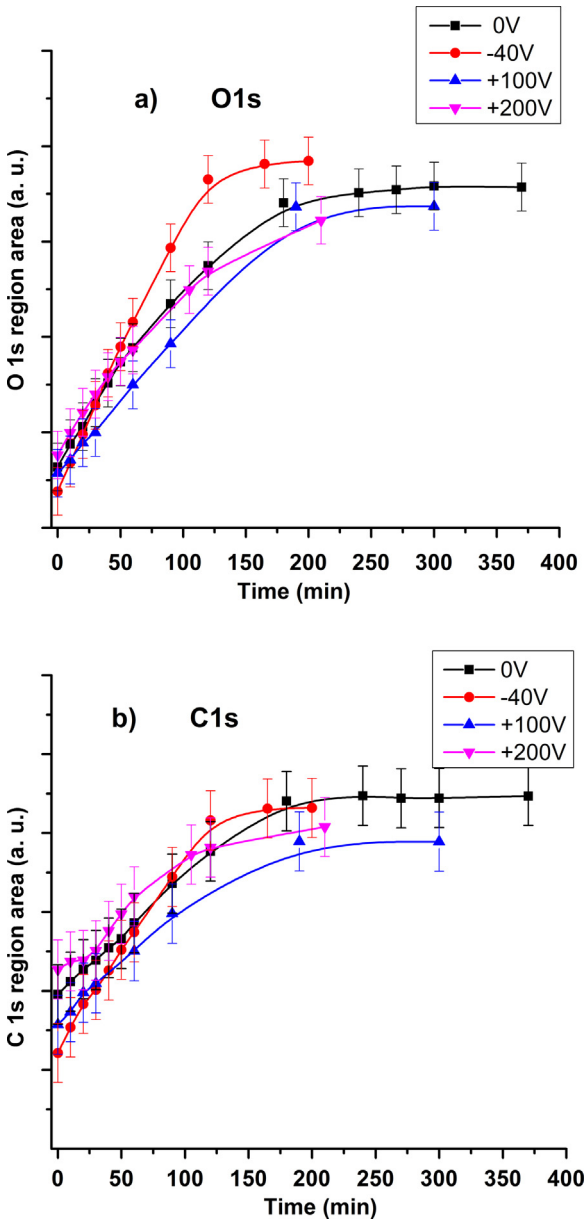

Fig. 6. The temporal evolution of area under XPS spectrum of the O1s region (a) and C 1*s* (b) regions, showing the evolution of the surface concentration of oxygen (H_2O) and carbon under different surface bias voltage and polarity compared to the case of natural evolution without surface biasing (0 V)., surface was scanned in high vacuum atmosphere at $\sim 2.0 \times 10^{-8}$ Torr.

surface [30]. On the other hand, the accumulation of hydrocarbon molecules was not found to be affected by the sample bias voltage (Fig. 6(b)). Although biasing the surface negatively is expected to make the same effect as the electron bombardment in terms of negative surface charging, the adsorption rate in the case of negative surface biasing was found to be unaffected. The reason behind the enhanced surface adsorption rate in the case of electron bombardment is attributed to the combination of the negative surface charging and the positively charged gaseous molecules produced during the direct interaction between the electron beam and the gaseous molecules in the chamber atmosphere.

Our results show that the surface bias voltage (up to +200 V) is found to be harmless in terms of surface contamination based on adsorption process in high vacuum atmosphere. Furthermore biasing the top surface layer of the EUV optics could be a good solution to mitigate EUV generated photo-electrons, especially SE that might increase the risk of optics contamination in the future EUVL devices. More research should be conducted in this direction to explore the effect of the surface bias voltage of EUV multilayer mirrors (MLMs) on their optical properties such as EUV reflectivity. For example, biasing the Ru capping of Si/Mo MLM could alter the electrons–holes distribution homogeneity, which can lead to changes in optical properties of the Si–Mo interfaces.

4. Conclusions

We investigated the impact of 100 eV electron beam on the physisorption of hydrocarbons and water molecules on Au surfaces to simulate the effects of contaminants on the optical system performance in future EUV devices. A noticeable accumulation of H_2O and hydrocarbons contaminants on the top of clean Au mirror in high vacuum atmosphere was observed. This accumulation was explained by the natural accumulation due to the adsorption process. The rate of accumulation of H_2O and hydrocarbons on the top of Au surface was increased significantly when the surface was bombarded by 100 eV electrons. The observed increase in adsorption rate was proportional to the electron beam current. This phenomenon of enhanced physical adsorption due to electron bombardment was explained by the enhancement of the sticking coefficient due to the formation of temporal electrostatic force between the adsorbed molecules and the bombarded surface. Also we noticed a decrease in the activation energy for desorption of the adsorbates. This decrease is most likely occurs due to the SE induced dissociation of larger molecules into smaller fragments, where less energy is required to desorb back to the gaseous phase.

In order to mitigate the electron induced enhanced adsorption of molecules, especially H_2O and hydrocarbons, we used biasing of the top mirror surface to suppress the surface SE emission generated during the EUV–surface interaction. Biasing the Ru mirror surface positively by 200 V was found to be useful to cut off more than 99% of the emitted electrons. On the other hand, we found that the positive biasing of Au surface does not have any influence on the rate of contaminants adsorption on the Au surface in high vacuum atmosphere. More research still needs to be conducted in order to understand the impact of applying positive bias voltage on the MLMs reflectivity.

Acknowledgment

This work was partially supported by College of Engineering, Purdue University and Department of Energy.

References

[1] L.R. Harriott, Proc. IEEE 89 (366) (2001).
[2] R.A. Lawes, Appl. Surf. Sci. 154–155 (519) (2000).
[3] T. Ito, S. Okazaki, Nature 406 (1027) (2000).
[4] B. Wu, A. Kumar, J. Vac. Sci. Technol. B 25 (1743) (2007).
[5] A. Al-Ajlony, A. Kanjilal, M. Catalfano, M. Fields, S.S. Harilal, A. Hassanein, J. Vac. Sci. Technol. B 30 (021601) (2012).
[6] A. Kanjilal, M. Catalfano, S.S. Harilal, A. Hassanein, B. Rice, J. Appl. Phys. 111 (063518) (2012).
[7] D. Seo, C. Park, J. Jung, M. Yoon, D. Lee, C.Y. Kim, S. Lim, Appl. Surf. Sci. 257 (10477) (2011).
[8] J. Hollenshead, L.E. Klebanoff, J. Vac. Sci. Technol. B 24 (64) (2006).
[9] K. Koida, M. Niibe, Appl. Surf. Sci. 256 (1171) (2009).
[10] A.B. Al-Ajlony, A. Kanjilal, S.S. Harilal, A. Hassanein, J. Vac. Sci. Technol. B 30 (041603) (2012).
[11] J. Hollenshead, L.E. Klebanoff, J. Vac. Sci. Technol. B 24 (118) (2006).
[12] A. Al-Ajlony, A. Kanjilal, M. Catalfano, S.S. Harilal, A. Hassanein, B. Rice, Proc. SPIE 8322 (832232) (2012).
[13] D.D. Do, Adsorption Analysis: Equilibria and Kinetics, Imperial College Press, London, 1998.
[14] I. Langmuir, J. Am. Chem. Soc. 40 (1361) (1918).
[15] S. Brunauer, P.H. Emmett, E. Teller, J. Am. Chem. Soc. 60 (309) (1938).
[16] H.F. Winters, D.E. Horne, E.E. Donaldson, J. Chem. Phys. 41 (2766) (1964).

[17] L.R. Danielson, M.J. Dresser, E.E. Donaldson, D.R. Sandstrom, Surf. Sci. 71 (615) (1978).
[18] H.D. Ebinger, J.T. Yates Jr., Phys. Rev. B 57 (1998) 1976.
[19] B.V. Yakshinskiy, R. Wasielewski, E. Loginova, T.E. Madey, Proc. SPIE 6517 (65172Z) (2007).
[20] B.V. Yakshinskiy, R.A. Bartynski, Proc. SPIE 7636 (76360F) (2010).
[21] S. Bajt, H.N. Chapman, N. Nguyen, J. Alameda, J.C. Robinson, M. Malinowski, E. Gullikson, A. Aquila, C. Tarrio, S. Grantham, Appl. Optics 42 (5750) (2003).
[22] T. Madey, N. Faradzhev, B. Yakshinskiy, N. Edwards, Appl. Surf. Sci. 253 (1691) (2006).
[23] M.J. van Staden, J.P. Roux, Appl. Surf. Sci. 44 (259–262) (1990).
[24] J.F. Moulder, W.F. Stickle, P.E. Sobol, K.D. Bomben, Handbook of X-Ray Photoelectron Spectroscopy, Perkin-Elmer Corporation, Eden Prairie, MN, 1992.
[25] J.P. Allain, M. Nieto, M.R. Hendricks, P. Plotkin, S.S. Harilal, A. Hassanein, Rev. Sci. Instrum. 78 (113105) (2007).
[26] R. Garg, A. Wüest, E. Gullikson, S. Bajt, G. Denbeaux, Proc. SPIE 6921 (692136) (2008).
[27] A. Egbert, B. Tkachenko, S. Becker, B.N. Chichkov, Proc. SPIE 5448 (693) (2004).
[28] Z.R. Yue, W. Jiang, L. Wang, S.D. Gardner, C.U. Pittman Jr., Carbon 37 (1785) (1999).
[29] A. Nikitin, H. Ogasawara, D. Mann, R. Denecke, Z. Zhang, H. Dai, K. Cho, A. Nilsson, Phys. Rev. Lett. 95 (225507) (2005).
[30] M.A. Henderson, Surf. Sci. Rep. 41 (1) (2002).